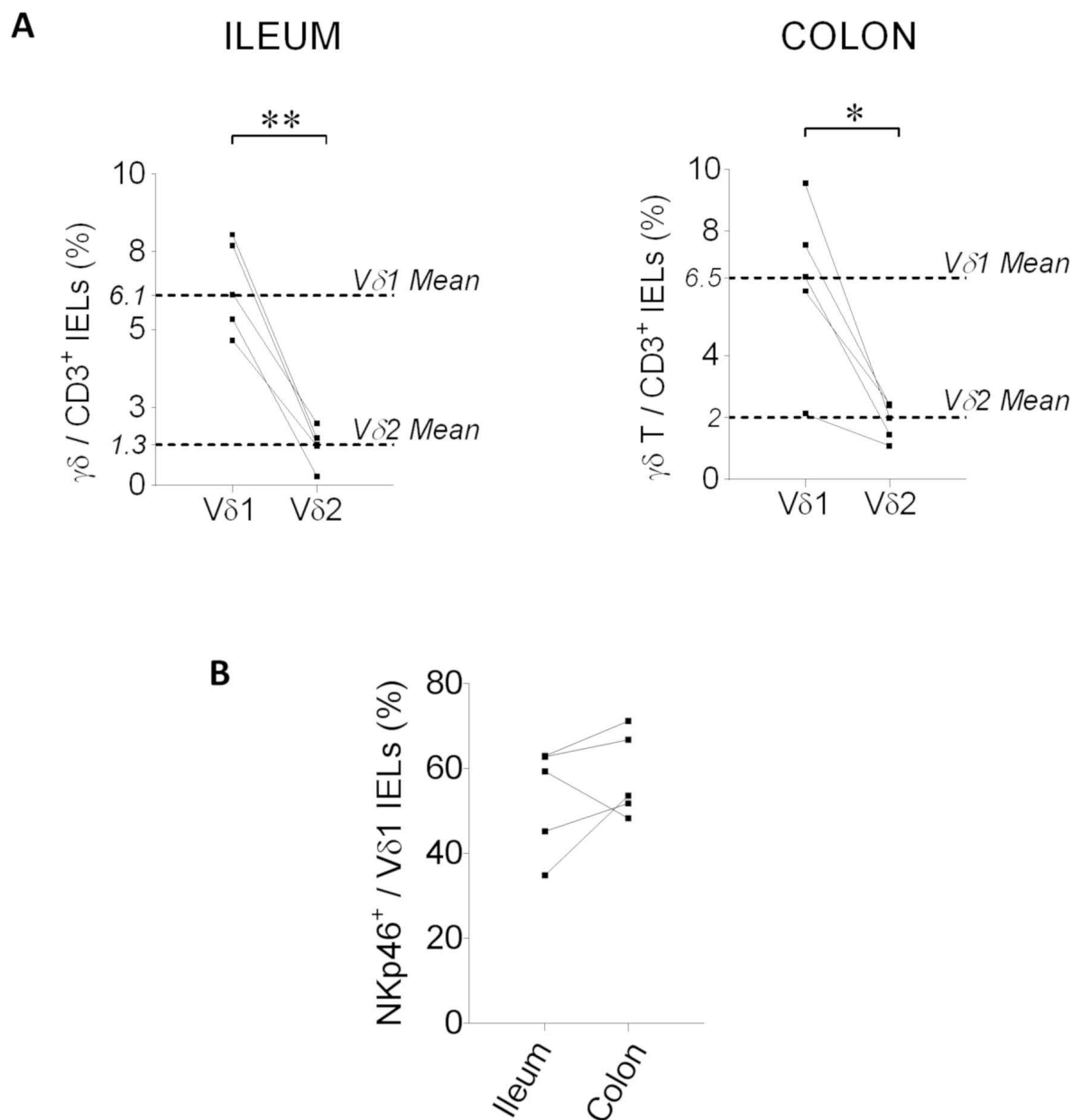


Legend Supplemental Figure 1.

Methodology and enrichment of NKp46^{pos} $\gamma\delta$ T cells within the crypts of healthy human intestine.

(A) Representative macroscopic examples of human intestine specimens in the presence (Tumor in a) and in the absence (Healthy in b) of intestinal adenocarcinoma. **(B)** Representative microscopic examples of a 4x hematoxylin-eosin staining showing specimens of intestine in the presence (Tumor in a) and in the absence (Healthy in b) of intestinal adenocarcinoma. **(C)** Representative examples of a 4x hematoxylin-eosin staining showing the specimens of healthy human intestine before (a) and after (b) the treatment with DL-Dithio-Threito (DDT) and Ethylene-Diamine-Tetra acetic Acid (EDTA) to specifically remove the epithelial crypts. The left tissue (b) was then enzymatically processed with collagenase II to obtain mononuclear cells from intestinal lamina propria. **(D)** Representative examples of contour plots showing the percentages of $\gamma\delta$ T cell within total CD45^{pos}/CD3^{pos} lymphocytes expressing NKp46 (upper line), NKp44 (middle line) and NKp30 (lower line) from both IEL and LPL compartments of an healthy gut specimen and from PBMC of an healthy donor. **(E)** Representative fluorescence microscopic image showing the expression within intestinal crypts of $\gamma\delta$ T (red on the far left image), CD3 (green on left image) and NKp46 (yellow on the right) markers alone and overlapped (merge on the far right image). Yellow arrows indicate fluorescent cells and DAPI in blue labels cell nuclei.

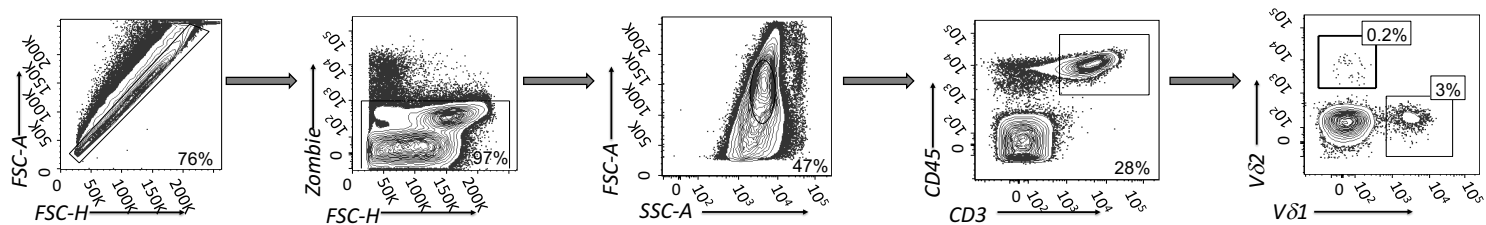


Legend Supplemental Figure 2.

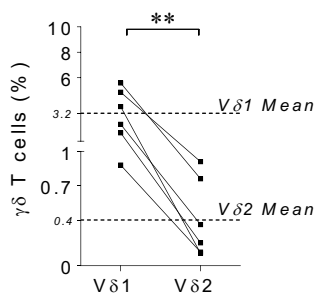
Frequency comparison of the NKp46^{pos}/Vδ1 subset in healthy human colon and ileum intraepithelial compartment.

(A) Summary statistical graphs showing the percentages of parallel Vδ1 and Vδ2 cells in CD45^{pos}/CD3^{pos} IELs in healthy human specimens of both ileum (left graph) and colon (right graph) intestinal compartments from Crohn's patients (N=5). (B) Summary statistical graph showing the frequencies of the specific NKp46^{pos}/Vδ1 IEL subset in matched healthy ileum and colon sections (N=5).

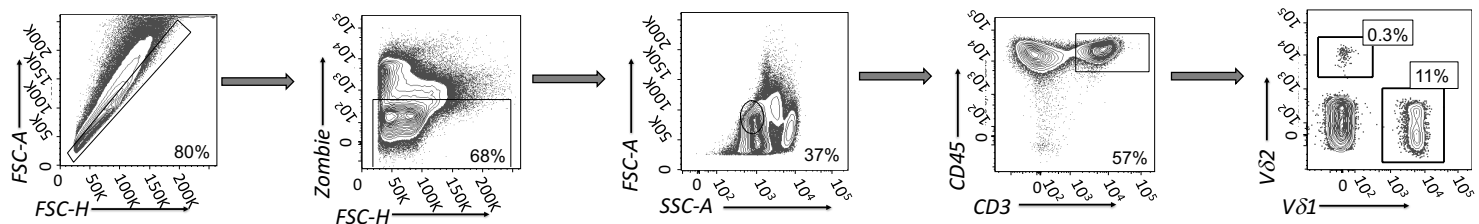
A



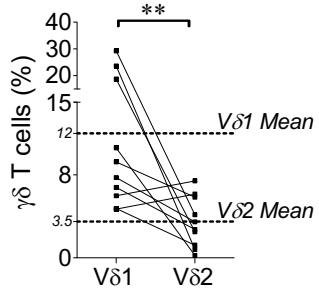
B



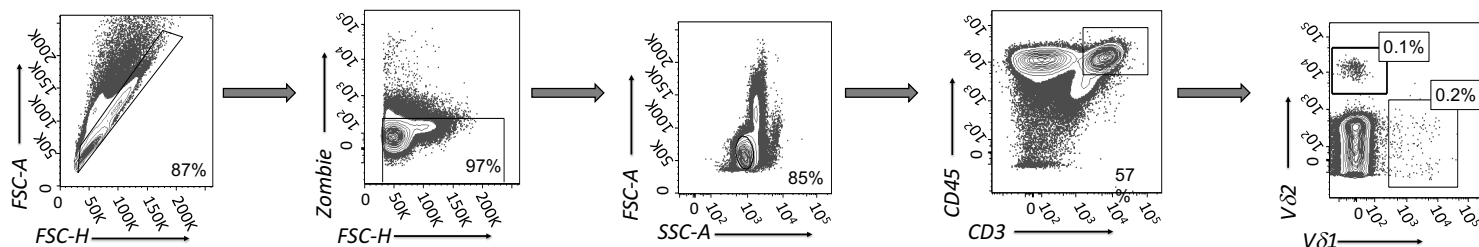
C



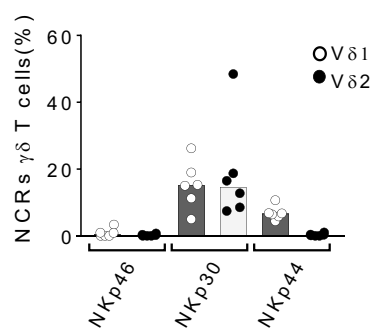
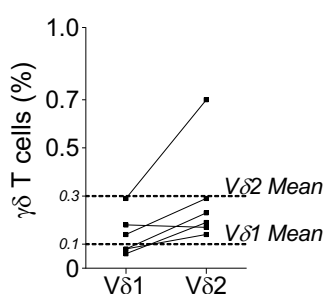
D



E



F



Legend Supplemental Figure 3.

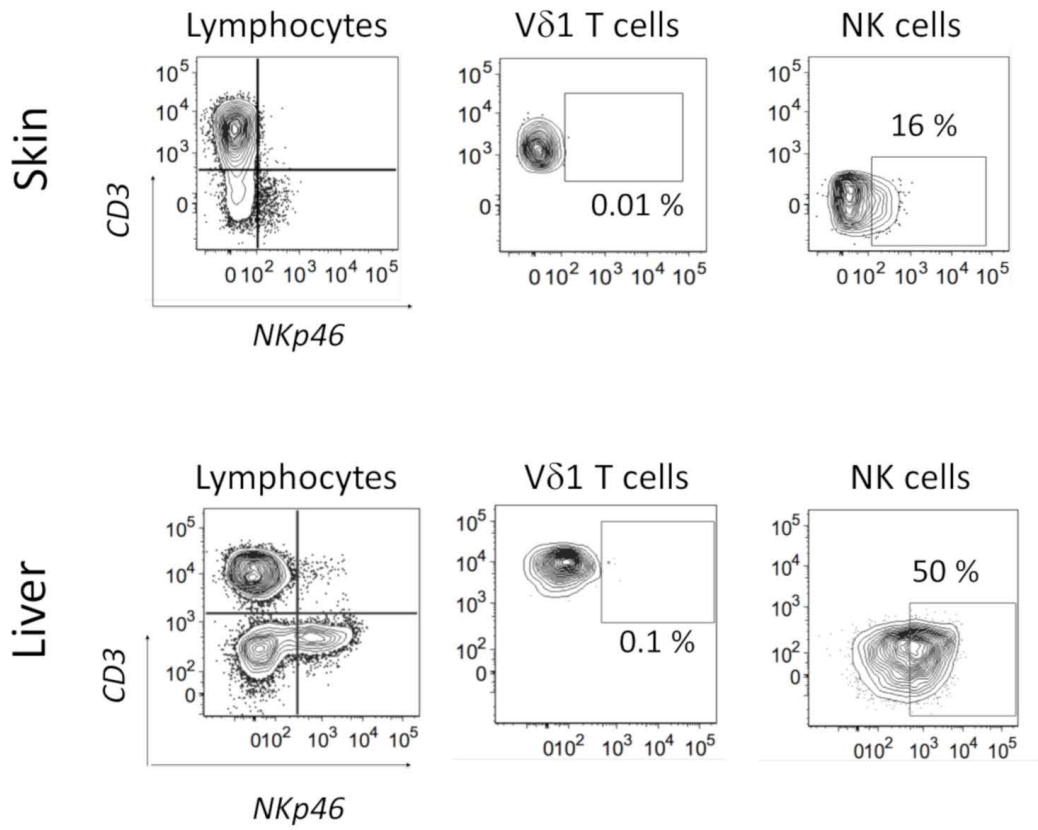
Frequencies of NCR^{pos} $\gamma\delta$ T cells in healthy human skin, liver and lymph nodes.

(A, C, E) Representative examples of flow cytometry dot plots showing the gating strategy used to identify viable CD45^{pos}/CD3^{pos} V δ 1 and V δ 2 lymphocyte subsets in specimens of healthy human skin (N=6) **(A)**, liver (N=9), **(C)**, and lymph node (N=6) **(E)**. **(B, D, F)**

Summary statistical graphs showing the percentages of V δ 1 and V δ 2 subsets (left graphs) in paralleled samples of healthy human skin **(B)**, liver **(D)** and lymph node **(F)**.

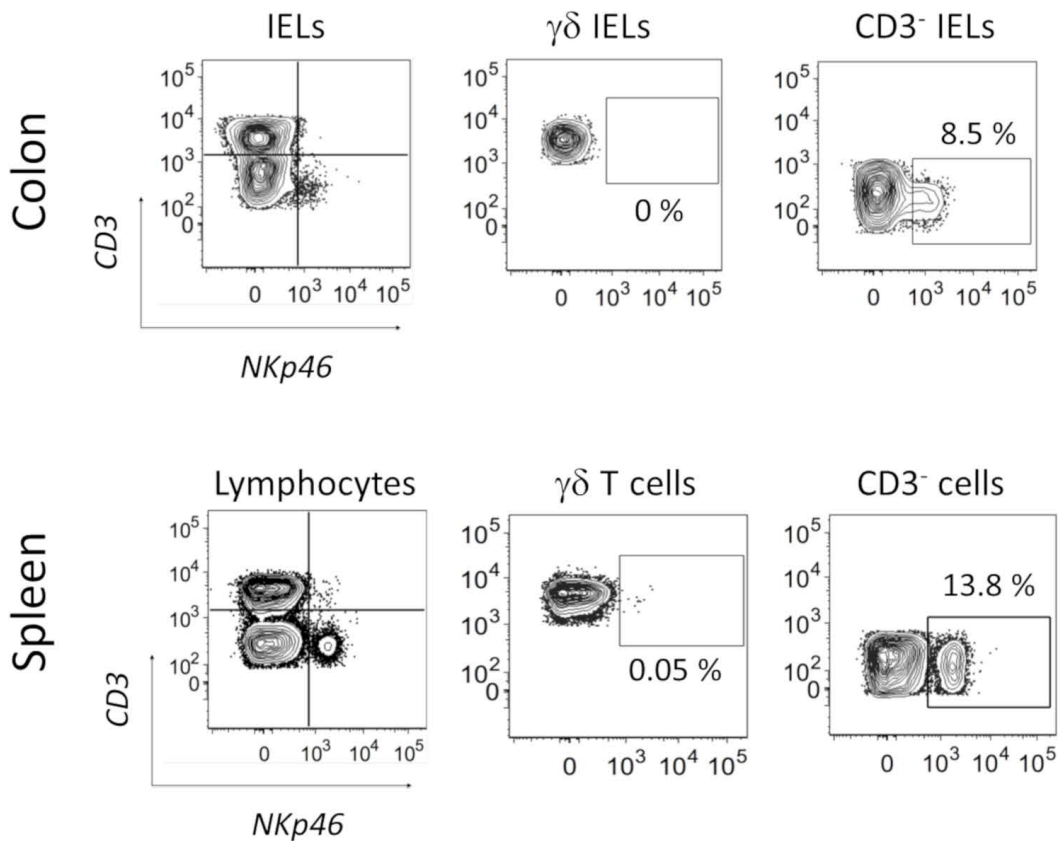
A

Human Tissues



B

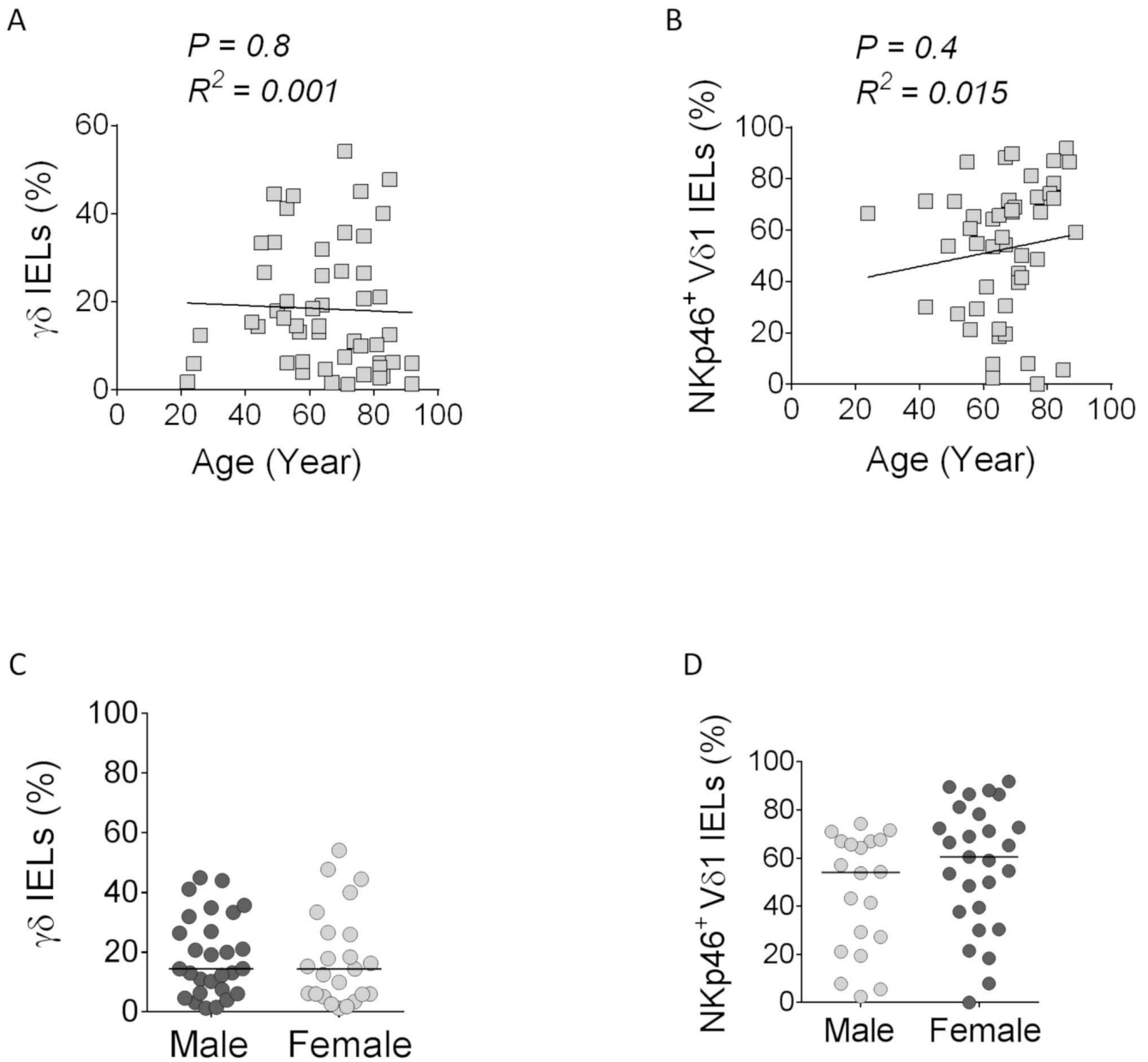
Murine Tissues



Legend Supplemental Figure 4.

Comparison expression of NKp46 in human and murine tissue-resident lymphocytes.

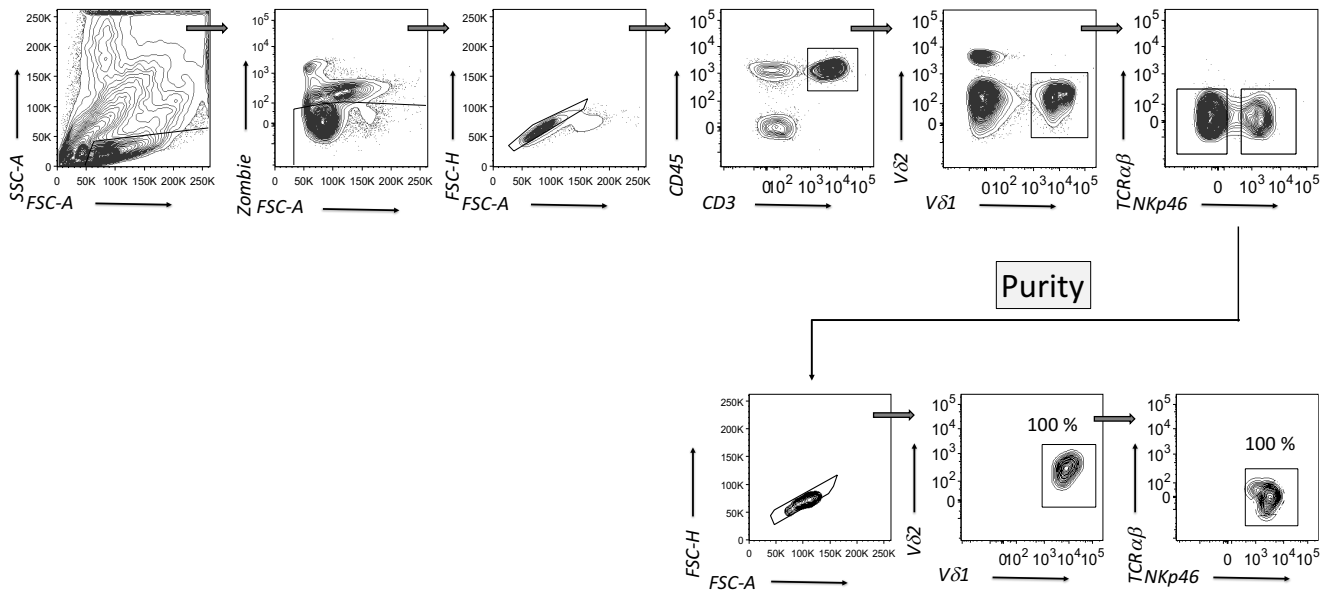
(A) Representative examples of flow cytometry dot plots showing expression of NKp46 on CD3^{pos} and CD3^{neg} T cells (left column), V δ 1 T cells (middle column) and CD3^{neg}/CD56^{pos} NK cells (right column) from the same human skin (upper line) and human liver (lower line) specimens. (B) Representative examples of flow cytometry dot plots showing in the same mice tissue specimens the expression of NKp46 on CD3^{pos} and CD3^{neg} IELs from colon (left column, upper plot) or CD3^{pos} and CD3^{neg} lymphocytes from spleen (left column, lower plot), on $\gamma\delta$ IELs from colon (middle column, upper plot) or $\gamma\delta$ T cells from spleen (middle column, lower plot), CD3^{neg} IELs from colon (right column, upper plot) or and CD3^{neg} cells from spleen (right column, lower plot).



Legend Supplemental Figure 5.

Impact of sex and age on the frequency of $\gamma\delta$ T cells and NKp46^{pos} V δ 1 cells within intraepithelial intestinal lymphocytes.

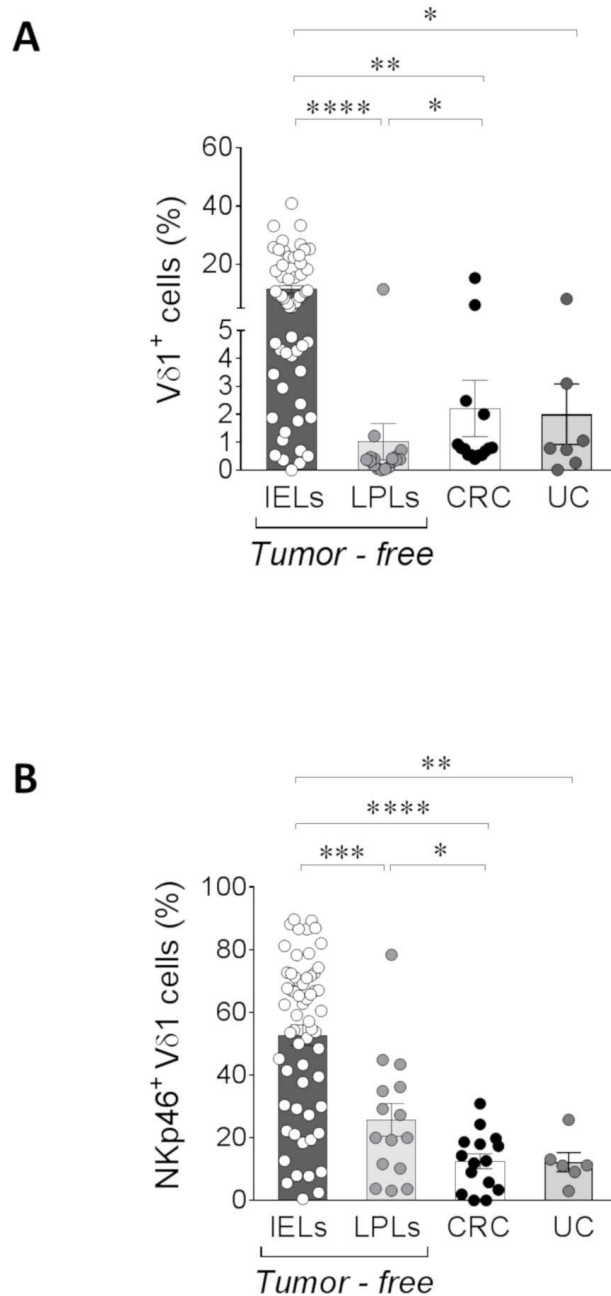
(A-B) Statistical analyses showing the correlation between the percentages of either $\gamma\delta$ IELs (A) or NKp46^{pos} V δ 1 (B) IELs and the age of donors enrolled in the study. (C-D) Summary statistical analyses showing the percentages of either $\gamma\delta$ IELs (C) or NKp46^{pos} V δ 1 (D) IELs in male and female donors enrolled in the study.



Legend Supplementary Figure 6.

Purity control of sorted human colon NKp46^{pos}/Vδ1 IELs.

Representative example of flow cytometry dot plots showing the gating strategy used to isolate and FACS-sort viable CD45^{pos}/CD3^{pos}/Vδ1^{pos}/αβT^{neg}/NKp46^{pos} IELs together with a purity control.



Legend Supplementary Figure 7.

Frequency of the NKp46^{pos}/V δ 1 subset in the pathogenesis of ulcerative colitis (UC).

(A-B) Statistical comparison of the incidence of tumor and inflammatory infiltrates of V δ 1^{pos} (A) and the specific NKp46^{pos}/V δ 1 cells (B) in tumor (CRC) (N=15) and ulcerative colitis (UC) patients (N=7) with the parallel V δ 1^{pos} and NKp46^{pos}/V δ 1 cells in healthy IEL and LPL compartments (N \geq 15).

Supplementary Table 1

Expression of NKp46 in mouse $\gamma\delta$ T lymphocytes.

Sample Tissue	Balb/c 5 weeks		C57BL/6 5 weeks	
	$\gamma\delta$ T	NKp46⁺ $\gamma\delta$ T	$\gamma\delta$ T	NKp46⁺ $\gamma\delta$ T
Colon (IELs)	3.7 % (± 0.28)	3.1 % (± 0.28)	10.3 % (± 0.66)	1.9 % (± 0.16)
Small Intestine (IELs)	53.7 % (± 1.41)	1.2 % (± 0.58)	32.7 % (± 0.77)	1.8 % (± 0.99)
Spleen (Splenocytes)	0.7 % (± 0.01)	4.1 % (± 0.22)	0.9 % (± 0.02)	2.9 % (± 0.32)

Legend Supplemental Table 1.

Expression of NKp46 in mouse $\gamma\delta$ T lymphocytes.

Statistical analyses showing the percentage ($\pm SD$) of $\gamma\delta$ T cells on total CD3^{pos} T lymphocytes or either the percentage of the specific NKp46^{pos} subset on $\gamma\delta$ T cells isolated from murine colon and small intestine intraepithelial compartment (IELs), and from the spleen (Splenocytes).